

Published in final edited form as:

*Biochim Biophys Acta*. 2012 January ; 1823(1): 15–28. doi:10.1016/j.bbamcr.2011.06.007.

## ClpXP, an ATP-powered unfolding and protein-degradation machine

Tania A. Baker<sup>1,2</sup> and Robert T. Sauer<sup>1,\*</sup>

<sup>1</sup>Department of Biology, Massachusetts Institute of Technology, Cambridge, Massachusetts, USA 02139

<sup>2</sup>Howard Hughes Medical Institute, Massachusetts Institute of Technology, Cambridge, Massachusetts, USA 02139

### Abstract

ClpXP is a AAA+ protease that uses the energy of ATP binding and hydrolysis to perform mechanical work during targeted protein degradation within cells. ClpXP consists of hexamers of a AAA+ ATPase (ClpX) and a tetradecameric peptidase (ClpP). Asymmetric ClpX hexamers bind unstructured peptide tags in protein substrates, unfold stable tertiary structure in the substrate, and then translocate the unfolded polypeptide chain into an internal proteolytic compartment in ClpP. Here, we review our present understanding of ClpXP structure and function, as revealed by two decades of biochemical and biophysical studies.

### 1. ClpXP is an archetypal AAA+ proteolytic machine

AAA+ enzymes utilize the energy of ATP binding and hydrolysis to perform the mechanical work required to power numerous biological reactions and processes [1]. An important subfamily of AAA+ machines function in ATP-dependent protein degradation in cells ranging from bacteria to humans [2]. Here, we review the structure, biological function, and molecular properties of ClpXP, a relatively simple and well-characterized AAA+ protease, which serves a paradigm for other ATP-dependent proteases, including ClpAP, ClpCP, HslUV, Lon, FtsH, PAN/20S, and the 26S proteasome.

ClpXP consists of two distinct proteins, a AAA+ ATPase called ClpX and a peptidase called ClpP. ClpX recognizes unstructured peptide sequences (called tags or degrons) in protein substrates, proceeds to unfold stable tertiary structure in the protein, and then spools or translocates the unfolded polypeptide chain into a sequestered proteolytic compartment in ClpP for degradation into small peptide fragments (Fig. 1). Irrespective of the biological source, ClpX is active as a ring hexamer, whereas ClpP is active as a 14-subunit self-compartmentalized peptidase. In this review, we focus principally on ClpXP from *Escherichia coli*, which has been characterized extensively and was the first ClpX-family protease to be isolated and studied.

© 2010 Elsevier B.V. All rights reserved.

\*corresponding author: address, MIT 68-571, Cambridge, MA, USA 02139; bobsauer@mit.edu; phone, 617-253-3163; fax 617-258-0673.

#### 9. Conflict of interest statement

The authors declare no conflict of interest.

**Publisher's Disclaimer:** This is a PDF file of an unedited manuscript that has been accepted for publication. As a service to our customers we are providing this early version of the manuscript. The manuscript will undergo copyediting, typesetting, and review of the resulting proof before it is published in its final citable form. Please note that during the production process errors may be discovered which could affect the content, and all legal disclaimers that apply to the journal pertain.

## 2. Discovery and early studies

The early history of ClpXP is intertwined with that of ClpAP, a different AAA+ protease that was initially purified in the late 1980's [3–5]. ClpAP consists of an ATPase (ClpA) and a separate peptidase (ClpP). By itself, ClpP digests small peptides but has no significant activity against proteins. Importantly, degradation of protein substrates requires ClpA, ClpP, and ATP hydrolysis. In the early 1990's, several groups discovered that ClpP could also function with a different AAA+ ATPase, ClpX, to carry out ATP-dependent proteolysis on substrates such as  $\lambda$ O, a phage replication protein [6–7]. The specificities of ClpXP and ClpAP differed, suggesting that the AAA+ components of these proteases were responsible for recognizing substrates. As we discuss below, this principle is now well established. Indeed, a few years later, ClpX alone was purified as an enzyme that removed MuA transposase from DNA following site-specific recombination [8–9]. Thus, ClpX can function as an ATP-dependent disassembly chaperone in the absence of ClpP. Occasionally, ClpX is present but ClpP is absent in an organism, suggesting that remodeling is the main function of ClpX in these species.

## 3. ClpX structure and function

The biochemical functions of ClpX include binding substrates, adaptors, and ClpP, protein unfolding, and polypeptide translocation. Unfolding and translocation require ATP binding and hydrolysis to power the changes in enzyme conformation that drive these mechanical processes. Moreover, for ClpX to productively bind ClpP and some substrates, ATP binding but not hydrolysis is required [10–14].

### 3.1 Domain and hexamer structures

Subunits of ClpX contain a family-specific N-terminal domain and a AAA+ module, consisting of large and small AAA+ domains (Fig. 2). The N domain folds independently of the AAA+ module as a dimer (Fig. 2B), with each subunit stabilized by coordination of a zinc atom [15–17]. The large and small AAA+ domains function together in hexameric rings, although the orientation between these domains can vary substantially in different subunits [18]. In the conformation shown in Fig. 2C, ATP or ADP binds in a cleft between the large and small AAA+ domains [18–19]. This cleft is largely formed by conserved sequence motifs (Walker A, Walker B, arginine finger, sensor-II arginine, etc.) that define the AAA+ superfamily [18–21]. Both full-length ClpX and ClpX <sup>$\Delta$ N</sup>, which consists only of the large and small AAA+ domains, form ring hexamers [10,18,22]. Importantly, ClpX <sup>$\Delta$ N</sup> binds ClpP with near wild-type affinity and supports ATP-dependent degradation of some native protein substrates at rates similar to wild-type ClpXP, demonstrating that the AAA+ domains perform the mechanical functions of ClpX [15,22–24]. N-domain dimers, which are flexibly tethered to the AAA+ ring of ClpX, are needed for recognition of adaptors and some substrates and contribute to hexamer stability [15,22].

The structures of the large and small AAA+ domains were initially determined in ADP-bound subunits of *Helicobacter pylori* ClpX <sup>$\Delta$ N</sup>, which formed continuous spirals in the crystal lattice [19]. Subsequent crystal structures of *E. coli* ClpX <sup>$\Delta$ N</sup> variants, in which some subunits were covalently linked, established the detailed conformation of ring hexamers (Fig. 3A & 3B) [18]. In nucleotide-free (apo) and nucleotide-bound ClpX <sup>$\Delta$ N</sup> hexamers, the conformations of the large and small AAA+ domains are essentially invariant and similar to those observed in the spiral structure. However, the hexamer structures contain two major classes of subunits that differ in domain-domain orientation. In four “loadable” or L subunits, the large and small AAA+ domains are oriented in nucleotide-binding conformations (Fig. 2C) similar to the one observed in the spiral structure. Strikingly, however, in two “unloadable” or U subunits, rotations of  $\sim 80^\circ$  between the large and small

AAA+ domains result in movements as large as 30 Å that destroy the nucleotide-binding site. The combination of nucleotide-binding competent and non-competent ClpX subunits in an L-L-U-L-L-U pattern results in a highly asymmetric hexameric ring (Fig. 3A & 3B) [18]. As we discuss below, there is strong experimental support that ClpX rings function as asymmetric hexamers, which can bind a maximum of four molecules of ATP and/or ADP.

When viewed from the top of a ClpX ring, each small AAA+ domain packs against the large AAA+ domain of the clockwise neighboring subunit in an essentially invariant fashion [18]. Each of these rigid-body interactions buries ~2000 Å<sup>2</sup> of surface area, providing the major subunit-subunit interactions that stabilize the ClpX ring. Thus, the ring can be viewed as six rigid-body units connected by a short hinge region between the large and small AAA+ domains of each subunit (Fig. 3C & 3D). As a consequence, the ring conformation is determined by the invariant geometry of each rigid body and by the detailed structure of the intervening hinge regions. For the loadable subunits, ATP/ADP binding and hinge conformation are related because nucleotide contacts are made by both AAA+ domains and the hinge, and the energetic coupling between these contacts depends on the precise hinge structure (Fig. 3E). Moreover, because the ClpX ring is topologically closed, changes in the orientations of the large and small domains in a single subunit, caused by ATP binding and/or hydrolysis, could easily propagate around the entire ring to help drive substrate unfolding and/or translocation.

## 4. Recognition of protein substrates

### 4.1 Direct recognition

ClpX recognizes protein substrates by binding to short unstructured peptide sequences, which are called degradation tags, degrons, or recognition signals. For example, C-terminal residues of the bacteriophage Mu repressor, the MuA transposase, and the RecN repair protein target these proteins to ClpX, and transfer of these residues to other proteins transfers susceptibility to ClpXP degradation [25–27]. Similarly, ClpXP degrades proteins that contain the *E. coli* *ssrA*-tag sequence at their C terminus [28]. When ribosomes stall during protein synthesis in eubacteria, the *ssrA* tag is added to the incomplete nascent protein by the tmRNA system, ensuring degradation of these molecules [29–30]. Importantly, appending the *ssrA* tag to a wide variety of model proteins via cloning has allowed biochemical and biophysical investigations of the influence of substrate structure and stability on the rate of ClpXP degradation [11,31–36]. The *E. coli* *ssrA* tag is 11 residues in length, but just two C-terminal alanines and the negatively charged  $\alpha$ -carboxyl group (AA-COOH) are the principal determinants of ClpX recognition [11,37]. As we discuss below, other residues in the *ssrA* tag mediate binding to the SspB adaptor, which aids in the delivery of *ssrA*-tagged proteins for ClpXP degradation [37–38].

In proteomic studies, endogenous *E. coli* substrates were initially trapped in the proteolytic chambers of inactive ClpXP proteases *in vivo* and were then purified and identified *in vitro* [27,39]. Five classes of ClpXP degradation tags were established by bioinformatics analysis of the trapped sequences, peptide-blotting experiments, tag-transfer experiments, and mutational studies (Fig. 4). Two classes of C-terminal targeting signals share homology with the *ssrA*-tag and MuA-tag sequences, respectively. One class of N-terminal degrons was similar to a sequence that targets the  $\lambda$ O protein for ClpXP degradation [40], whereas another N-terminal class included signal sequences for protein secretion [39]. Apparently, failure of normal secretion results in cytoplasmic degradation by ClpXP.

Some degradation tags bind in the axial pore of ClpX. For example, the *ssrA* tag can be crosslinked to the pore-1 and pore-2 loops within the axial channel of the ClpX ring [41]. Similarly, mutations in both of these pore loops increase  $K_M$  and decrease apparent ClpXP

affinity for *ssrA*-tagged substrates [24,42–43]. A set of flexible ClpX loops, which surround the entrance pore and contain an RKH sequence, also play important roles in tag recognition (Fig. 5A). The importance of these loops in substrate recognition is dramatically illustrated by the fact that human ClpX, which contains the same GYVG loop as *E. coli* ClpX, fails to recognize the *ssrA* tag, but a variant with transplanted pore-2 and RKH loops from *E. coli* ClpX acquires this activity (Fig. 5B) [41]. Moreover, mutations that reduce the positive charge of the RKH motif weaken binding of *E. coli* ClpX to the negatively charged  $\alpha$ -carboxylate of the *ssrA* tag (Fig. 5C & 5D) [44]. Strikingly, the same mutations cause better binding to substrates with positively charged degradation tags (Fig. 5C & 5D), including the N-terminal  $\lambda$ O recognition tag and the C-terminal MuA tag [44]. These results suggest that the substrate specificity of wild-type ClpX is an evolutionary compromise that allows recognition of many different types of substrates but has not been optimized for any single protein or class of substrates. Compromises of this type are probably common for proteases and chaperones that interact with a large number of radically different substrate and client proteins. More than 100 intracellular substrates have been identified for ClpXP [27,39].

Although the N domain of ClpX is dispensable for degradation of *ssrA*-tagged proteins, it plays a critical role in recognition of some substrates. For example, removal of the N domain completely abrogates degradation of the  $\lambda$ O protein [15,22]. The N domain is also required for degradation of the UmuD' subunit of UmuD•D', a translesion DNA polymerase [45–46]. In this case, tethering interactions between the N domain and sequences in the UmuD subunit facilitate engagement of a tag in the UmuD' subunit by the pore of the ClpX ring. The N domain plays an interesting role in ClpX interactions with the MuA transposase. Phage Mu replication requires ClpX disassembly of transpososomes, which consist of a MuA tetramer bound to recombined DNA [8–9,47]. MuA has a C-terminal tag that targets monomers for degradation by ClpXP and is also required for tetramer disassembly by ClpX [26]. ClpX $\Delta$ N supports ClpP degradation of MuA monomers at near wild-type rates, consistent with recognition of the MuA tag by the ClpX pore [48]. Strikingly, however, ClpX $\Delta$ N fails to support Mu replication *in vivo* [15] and displays a dramatic defect in transpososome disassembly *in vitro*, caused by poor tetramer recognition [48]. Together, these results suggest that transposase disassembly requires engagement of the MuA C-terminal tag by the axial pore of ClpX, in addition to recognition of additional MuA sequences that are only exposed in the DNA-bound tetramer by the N domain of ClpX [48].

## 4.2 Adaptor-mediated substrate recognition

Two adaptor proteins, SspB and RssB, work in concert with ClpXP to modulate proteolysis of specific substrates. SspB helps deliver *ssrA*-tagged proteins and additional substrates for ClpXP degradation [38,49], whereas RssB is a two-component response regulator that controls degradation of  $\sigma^S$ , the *E. coli* stationary-phase transcription factor [50–51]. Because the molecular mechanisms of SspB delivery are better understood, we focus on this system below.

SspB was initially purified as an activity that specifically enhanced ClpXP degradation of *ssrA*-tagged proteins, predominantly by lowering  $K_M$  [38]. Several features of this adaptor allow it to tether substrates to ClpX and thus to deliver them for degradation. First, each subunit of the SspB dimer contains a groove that binds to an N-terminal sequence of the *ssrA* tag, adjacent to the C-terminal segment recognized by ClpX (Fig. 6A) [12,37,52–53]. Second, each SspB subunit has a highly flexible C-terminal tail that ends in a sequence that docks with the N domain of ClpX [15,17,54–57]. Both tails of the SspB dimer are needed for high-affinity tethering of *ssrA*-tagged substrates to ClpX and for efficient stimulation of ClpXP degradation [56], indicating that SspB makes multivalent contacts with a ClpX hexamer during substrate delivery.

An *ssrA*-tagged substrate can be bound to SspB and simultaneously engaged by ClpX. For example, after covalently attaching the tag to SspB via an engineered disulfide bond, this complex was found to bind ClpX much more tightly than SspB alone or the tag alone [58]. Thus, the C-terminal residues of the *ssrA* tag must contact ClpX at the same time that its N-terminal residues bind SspB. The individual binary contacts that stabilize the ternary complex of ClpX, SspB, and an *ssrA*-tagged substrate are relatively weak. However, avidity or effective-concentration effects ensure that a combination of these contacts results in very strong binding. For example, each SspB tail binds to an N domain with  $\sim 20 \mu\text{M}$  affinity, the *ssrA* tag binds to the ClpX pore with an affinity of  $\sim 1 \mu\text{M}$ , and the combination of all three contacts results in  $\sim 15 \text{ nM}$  binding of ClpX to the SspB-substrate complex [12,56–58]. Given the normal intracellular concentrations of ClpXP and SspB (100–150 nM), this tight affinity would ensure efficient degradation of *ssrA*-tagged substrates present in only a few copies per cell.

How is this stable delivery complex disrupted to begin substrate degradation? Strikingly, when the tag of GFP-*ssrA* was disulfide bonded to SspB, ClpXP degraded both GFP and the covalently attached adaptor (Fig. 6B) [58]. Thus, to resolve the normal adaptor-substrate complex, it appears that ClpX pulls on the *ssrA* tag, thereby initiating degradation and simultaneously breaking contacts with SspB.

In addition to *ssrA*-tagged substrates, proteomic experiments revealed that SspB also stimulates ClpXP degradation of N-RseA, an N-terminal fragment of a transmembrane protein [49]. During the *E. coli* envelope-stress response, RseA is cleaved by membrane proteases, releasing a complex of N-RseA and the  $\sigma^E$  transcription factor from the membrane [59]. ClpXP, aided by SspB, then degrades the N-RseA portion of this complex, freeing  $\sigma^E$  to activate transcription of stress genes [60]. Like *ssrA*-tagged proteins, N-RseA has a C-terminal AA-COOH degron that targets it to ClpX [49]. Surprisingly, however, the portion of N-RseA that binds SspB shows no sequence similarity with the region of the *ssrA* tag that binds SspB. Moreover, the segment of N-RseA that binds SspB interacts with the peptide groove in an orientation opposite that of the *ssrA* tag and makes only a single common contact when the two cocrystal structures are compared [61]. Thus, SspB can deliver very different types of substrates for ClpXP degradation.

At low substrate concentrations, SspB enhances the rate of ClpXP proteolysis of *ssrA*-tagged proteins or RseA  $\sim 10$ -fold but can stimulate degradation of model substrates with weak degradation tags to a far greater extent [38,49,62–63]. For example, mutating the C-terminal residues of the *ssrA* tag to bind more weakly to the ClpX pore resulted in weak- $K_M$  substrates that were degraded  $\sim 100$ -fold faster in the presence than absence of SspB [62]. Indeed, such substrates accumulated in *E. coli* when SspB levels were very low, but were degraded rapidly upon induction of high-level SspB expression (Fig. 7). Similar systems, using SspB stimulation of ClpXP degradation of substrates with inherently weak degradation tags, have been successfully used in *Bacillus subtilis*, *Mycobacterium smegmatis*, and *Mycobacterium tuberculosis* as a means of interrogating function by rapidly removing specific proteins from the cell [64–65] and are likely to work in any bacterium that contains ClpXP. Simple tethering of substrates to ClpXP raises their effective concentration relative to the pore and is sufficient for adaptor function, as synthetic split-adaptors that associate in the presence of rapamycin mimic substrate delivery by wild-type SspB and can be used to direct biological degradation [66].

### 4.3 Control of cellular protein levels by degradation

ClpXP degradation contributes to control of cellular protein levels in many ways. For quality control of protein synthesis, ClpXP is responsible for degrading most substrates produced by tmRNA-mediated addition of the *ssrA* tag during failed ribosomal translation



[28–30,68–69]. This problem is significant, as approximately 1 of every 200 protein-synthesis events in *E. coli* terminates with *ssrA* tagging [67]. Once tagging occurs, there is sufficient intracellular ClpXP (~100 molecules) and SspB (~120 molecules) to ensure rapid degradation of the tagged proteins [68]. For example, when the N-terminal domain of  $\lambda$  repressor, which normally has a half-life of many hours, was modified by intracellular *ssrA* tagging, the half-life of the tagged protein was ~0.5 min in cells containing SspB and ~5 min in cells lacking SspB [38]. Because of the limited number of ClpXP proteases in cells, however, the capacity for degradation of *ssrA*-tagged substrates can be easily overwhelmed by over production of a genetically tagged protein. Indeed, most of the *ssrA*-tagged substrates that our labs use for biochemical studies are over expressed and purified from cells containing wild-type ClpX, ClpP, and SspB.

Certain stress-response proteins contain degradation tags that result in efficient ClpXP degradation and need to be synthesized at high levels to maintain significant cellular concentrations. For example, *E. coli* RecN is a repair protein with an AA-COOH degron that targets it to ClpXP [27]. When DNA damage induces the SOS transcriptional response, high levels of *recN* mRNA and protein are synthesized, allowing RecN to accumulate despite constitutive ClpXP degradation. Once DNA-damage triggered SOS transcription ceases, however, ClpXP degradation rapidly reduces RecN levels in the cell. This intrinsic instability of cellular stress-response proteins appears to be a common theme, allowing the proteome to rapidly return to the pre-stressed state and ensuring degradation of proteins that are important for fighting stress but are also deleterious or mildly toxic [27,45–46,70].

For ribosomes and many large macromolecular complexes, it appears to be common that degrons recognized by ClpXP are exposed only in unassembled subunits [27,39]. When degrons are inaccessible in a native structure or buried in a protein-protein interface, it is straightforward to imagine how unfolding or post-translational modifications could be used to reveal these cryptic degrons. For example, ClpXP only degrades Fnr repressor under aerobic conditions in which oxidation destroys an iron-sulfur cluster that is important for dimer stability, thereby promoting dissociation and access to degradation signals in the monomer [71]. Fnr monomers contain two sequences that target it for degradation by ClpXP. Similarly, among the ClpXP substrates identified by proteomics, ~25% contained at least two predicted degrons per polypeptide [27,39]. In some of these proteins, it is likely that efficient recognition by ClpXP requires binding to both degradation signals, allowing proteolysis to be controlled by binding or folding events that modulate the exposure of these sequence tags.

## 5. ClpP structure and function

The only positive biological function of ClpP is to serve as the proteolytic component of ClpXP, ClpAP, or related AAA+ proteases. In this role, ClpP simply needs to bind its partner ATPase and to cleave any polypeptide that is translocated into its proteolytic chamber. The size of the resulting peptide fragments must be small enough to exit the chamber and subsequently be degraded by exopeptidases to free amino acids. In addition, the free ClpP enzyme must not function as an efficient protease. The importance of this “negative” role is highlighted by the biological activity of acyldepsipeptide antibiotics, which kill bacteria by binding ClpP and facilitating degradation of nascent chains and other unfolded polypeptides [72–73].

*E. coli* ClpP is expressed as a proenzyme [74]. Autoproteolysis subsequently removes a 14-residue N-terminal propeptide to generate the mature sequence of 193 amino acids. The three-dimensional structure of ClpP, observed initially at low resolution by electron microscopy (EM) [75–76] and shortly thereafter at atomic resolution by X-ray

crystallography [77], provided an elegant and straightforward explanation for its for its inactivity against protein substrates but its ability to degrade small peptides. Specifically, the proteolytic active sites of ClpP reside within a barrel-shaped chamber, formed by the face-to-face stacking of two heptameric ClpP rings (Fig. 8A). Small axial pores in each ClpP ring provide an opening into the proteolytic chamber. The dimensions of these pores in free ClpP (Fig. 8B) are large enough to allow small peptides to enter the chamber but small enough to exclude folded proteins and to dramatically slow the entry of large unfolded polypeptides [77].

Early studies revealed that the peptidase activity of ClpP was inhibited by diisopropylfluorophosphate [5,78–79], which covalently modifies the active site of serine proteases. In addition, the first crystal structure of *E. coli* ClpP showed that each subunit harbored a classical Ser-His-Asp catalytic triad and oxyanion hole, with conformations expected for a functional serine protease [77]. Subsequent structures of ClpP from *E. coli* and *Helicobacter pylori* were solved with a bound peptide inhibitor or product [80–81]. In these structures, the P1 side chain of the substrate mimic (representing the position immediately N terminal to the cleaved peptide bond) binds in a spacious hydrophobic pocket, and the peptide backbone of residues P1–P4 forms  $\beta$ -sheet hydrogen bonds with ClpP (Fig. 8C). Although a wide variety of chemically dissimilar side chains can serve as P1 residues, non-polar residues are preferred [78,82]. For example, ~80% of products produced by ClpXP degradation of GFP-ssrA result from cleavage after Leu, Gly, Met, Ala, and Tyr [82]. Moreover, in peptide substrates that are cleaved very rapidly by ClpP alone, non-polar side chains are strongly preferred at the P1 position with some additional preferences at the P3 and P5 positions [78].

The proteolytic chamber of ClpP is roughly spherical (diameter ~50 Å) and, in principle, could accommodate several hundred residues of an unstructured substrate [77]. Two factors ensure efficient cleavage of polypeptides that enter the chamber. First, the local concentration of active sites is very high (~350 mM). Thus, simply proximity drives active-site binding and cleavage of even weakly interacting sequences. Second, each of the 14 active sites in the ClpP chamber is ~25 Å from three additional active sites (two in neighboring subunits in the same ring and one in the opposite ring), a distance that could be spanned by ~8 substrate residues in an extended conformation. Thus, a polypeptide in the degradation chamber could simultaneously bind to multiple active sites, increasing avidity and tandem-cleavage events. The fastest reported ClpP cleavage of a peptide substrate occurs at a rate of ~10,000 min<sup>-1</sup> ClpP<sub>14</sub> [78]. This cleavage rate combined with an average product size of ~10 residues would be more than sufficient to prevent accumulation of substantial quantities of unfolded substrate in the ClpP chamber, as the ClpX translocation rate is substantially slower [36].

As noted above, the molecular architecture of ClpP limits the activity of the isolated enzyme to degradation of small peptides, and ClpP alone cleaves unstructured polypeptides larger than 20–30 residues very slowly [78,83]. This size restriction is enforced by the size of the axial channel, determined in part by residues 1–21 of mature ClpP (Fig. 8B), which form stem-loop structures that comprise the channel walls [77,80–81,84–87]. Although these stem-loop structures are visible in only some ClpP crystal structures, mutation of these residues allows degradation of larger peptides and unfolded proteins [83,88]. Importantly, structures of ClpP in complex with acyldepsipeptides revealed conformational changes that resulted in a much wider axial channel (~20 Å; Fig. 8D), explaining why these antibiotics result in ClpP degradation of large unfolded polypeptides [89–90].

ClpP orthologs are widespread throughout eubacteria and in the mitochondria and chloroplasts of many eukaryotic cells [91]. The active form of all ClpP orthologs is a

double-ring tetradecamer. Single heptameric rings, which are likely to be assembly/disassembly intermediates, are observed under some conditions [92,93]. For example, the principal solution species formed by human ClpP is a single ring [93], although double-ring tetradecamers are observed in a crystal structure and in complexes with its ClpX partner [84,93]. By itself, human ClpP cleaves small peptides poorly, suggesting that inactive heptamers equilibrate with active tetradecamers, which in turn are stabilized by ClpX binding. The inactivity of single rings, despite exposure of the proteolytic sites, would prevent rogue degradation until the double-ring cage assembles and binds ClpX or ClpA.

ClpP tetradecamers adopt inactive as well as active conformations. For example, in some crystal structures of variants or orthologs, the active sites are malformed, part of a helix that forms the ring-ring interface is disordered, and the distance between axial pores is ~10 Å shorter than in “active” structures (Fig. 8E) [77,80,84–87,91,94]. Ligand-mediated positive cooperativity is observed in cleavage and activation experiments [79–80,89–90], suggesting that binding stabilizes a higher affinity conformation of ClpP. These changes may be similar to the smaller conformational differences observed between structures of “active” ClpP, ClpP bound to a peptide inhibitor, and ClpP bound to acyldepsipeptides. The ring-ring interface of ClpP also exchanges between distinct conformations in solution NMR experiments, potentially similar to those in the crystallographic expanded and compact structures [95]. This result led to the intriguing proposal that the egress of peptide products from the ClpP chamber does not involve the axial pores but rather occurs via windows that open transiently near the ring-ring interface [95].

## 6. Interaction of ClpX and ClpP

EM initially showed that hexameric ClpX rings stack coaxially onto one or both ends of the ClpP barrel to form singly- or doubly-capped structures [10]. In these complexes, the axial pores of the ClpX rings align with the pores in the ClpP rings, providing a route into the proteolytic chamber. Consistently, electron density for translocating substrates in the pore was visualized in some EM studies [96–97], and cysteines in a translocating substrate were shown to form disulfide crosslinks with cysteines introduced into the ClpX pore [24]. In doubly-capped ClpX<sub>6</sub>•ClpP<sub>14</sub>•ClpX<sub>6</sub> complexes, translocation at any given time appears to occur from only one of the two ClpX rings [97]. This result indicates that the two ClpX rings must coordinate their activities through ClpP.

A ClpX ring has six subunits and a ClpP ring has seven subunits, making a symmetry mismatch inevitable. Because high-resolution structures of ClpXP have not been solved, current models are based upon EM structures, modeling using crystal structures, and mutational and biochemical studies. The ClpXP complex appears to be stabilized by one set of interactions involving loops near the axial pores of each ring and another set between peripheral structural elements in the ClpX and ClpP rings (Fig. 9A). For example, the importance of axial contacts is indicated by destabilization of ClpXP complexes containing deletions or point mutations in the pore-2 loop of ClpX or in the N-terminal stem-loop residues of ClpP, by crosslinking studies, and by double-mutant experiments [24,84–85,88,98].

The peripheral ClpXP interactions involve docking of conserved sequences in surface ClpX loops with clefts on the faces of the ClpP barrel. Bioinformatic searches initially identified homologous tripeptides (IGF in *E. coli* ClpX) in a surface loop that was present in all ClpP-binding AAA+ ATPases [99]. IGF-loop mutations eliminate or weaken binding to ClpP without affecting other ClpX functions [13,99]. Moreover, chymotrypsin cleaves unbound ClpX hexamers immediately after the IGF sequence but does not cleave this site in the ClpXP complex [22]. Finally, engineered ClpX hexamers with just five IGF loops bind ClpP



with ~40-fold reduced affinity and variants with four IGF loops fail to bind [24]. The IGF loops are disordered in crystal structures of *E. coli* ClpX hexamers and have varied lengths in orthologs, suggesting a high degree of loop flexibility that could facilitate asymmetric connections between the mismatched rings of ClpX and ClpP [18,99]. The role of hydrophobic clefts on the faces of the ClpP<sub>14</sub> barrel as IGF-docking sites was initially suggested by modeling and confirmed by mutagenesis [86,99]. Acyldepsipeptides, which contain a phenylalanine residue, also bind in these clefts (Fig. 9B), apparently mimicking IGF binding (Fig. 9C) [73,89–90]. Both acyldepsipeptides and ClpX stimulate ClpP cleavage of peptides larger than a few amino acids, suggesting that IGF-loop binding in the ClpP clefts causes widening of the axial channel of the protease [24,73,83,89–90].

Tight binding of ClpX to ClpP requires ATP or the slowly hydrolyzed ATP $\gamma$ S analog and is enhanced modestly during substrate degradation [10,13,100]. Binding is not detected in the absence of nucleotide or with ADP. ClpX mutants bearing the E185Q mutation in the Walker-B motif fail to hydrolyze ATP but still show ATP-dependent binding to ClpP [14], demonstrating that ATP/ATP $\gamma$ S binding rather than hydrolysis activates ClpX for ClpP binding. However, ClpX hexamers with the sensor-II R370K mutation do not bind ClpP [13]. The side chain of Arg<sup>370</sup> is positioned to contact the  $\gamma$ -phosphate of ATP [18–19], apparently coupling nucleoside triphosphate binding to ClpX conformational changes needed for productive ClpP binding.

An important question is whether the conformation of ClpP changes in concert with ATP binding and hydrolysis by ClpX. Two models can be envisioned. (i) ClpX binding could stabilize an active proteolytic conformation of ClpP, which then remains relatively static during the ATP-fueled conformational changes that drive substrate denaturation and translocation. (ii) Changes in the conformations of the ClpX and ClpP ring could be coupled, helping to synchronize substrate translocation, degradation, and product release. Single-molecule FRET studies may be required to resolve this issue. It is clear, however, that ClpP binding influences ClpX function. For example, ClpP binding suppresses the rate of ATP hydrolysis by ClpX (an activity that depends on interactions made by the pore-2 loop), enhances the rate of ClpX unfolding of several substrates, and suppresses the degradation/unfolding defects of the D382K and L381K ClpX mutations, which affect rigid-body packing between adjacent subunits [13,18,24,99–100]. The degradation activity of ClpP is not required for these effects on ClpX function [13].

## 7. Nucleotide transactions

### 7.1 Steady-state ATP hydrolysis

The steady-state kinetic parameters for ClpX hydrolysis of ATP change as a function of the presence of ClpP and/or protein substrates [99,101]. Strikingly, however, changes in  $V_{\max}$  are linearly correlated with changes in  $K_M$ , as expected if most ATP molecules that bind ClpX leave the enzyme by hydrolysis and subsequent dissociation of ADP [101]. This model predicts that  $K_M$  for ATP hydrolysis should be much weaker than  $K_D$  for ATP binding. In fact,  $K_M$  values range from 80–400  $\mu$ M, whereas  $K_D$  for the hydrolysis-defective E185Q ClpX mutant is ~1  $\mu$ M [14,101]. Moreover, because ClpX hydrolyzes ATP $\gamma$ S at ~1/20 the rate of ATP, this model also explains why  $K_M$  for ATP $\gamma$ S hydrolysis (~10  $\mu$ M) is substantially lower than  $K_M$  for ATP hydrolysis [101].

At saturating concentrations of ATP, the hydrolysis rate per ClpX hexamer ranges from 100–600  $\text{min}^{-1}$ , depending on the presence of ClpP and/or protein substrates [34,101]. From the perspective of energy conservation in a cell, it may seem somewhat odd that ClpX and ClpXP hydrolyze ATP quite rapidly even when protein substrates are absent. Nevertheless, ClpX orthologs show similar behavior as do most other AAA+ unfoldases and proteases. If

these molecular machines are always working to degrade proteins in the cell, however, then there would be little evolutionary pressure for limiting the ATP-hydrolysis activity of substrate-free enzymes.

## 7.2 Asymmetric nucleotide interactions

As noted above, only four subunits in the ClpX hexamer can bind nucleotide in crystal structures [18]. Biochemical studies strongly support the conclusion that ATP binding to the hexamer is also highly asymmetric in solution. For example, the hydrolysis-defective E185Q variant of ClpX binds a maximum of four ATPs per hexamer [14]. The binding-competent sites in E185Q ClpX also differ in the kinetics of ATP dissociation, with some sites releasing ATP with a half-life of ~5 s and others displaying a substantially longer half-life [14].

Binding of the *ssrA* tag to the axial pore of ClpX is thermodynamically linked to the binding of ATP and  $Mg^{++}$  [14], and ~30-fold less ATP is required to support ClpX binding to a complex of SspB and an *ssrA* peptide than to support binding to the peptide alone. This difference correlates with the finding that the SspB-peptide complex binds ClpX much more tightly than the free *ssrA* peptide [58]. In these experiments, complex or *ssrA*-tag binding increases in a strongly cooperative manner as the ATP concentration is raised (Hill constant >2.6) [14]. Both ATP binding and the rate of hydrolysis also increase cooperatively with ATP concentration (Hill constants 1.4–1.6) [14]. Because Hill constants define the minimum number of ligand-bound sites needed to support activity, fewer ATP-bound ClpX subunits are likely to be needed to allow hydrolysis than to bind *ssrA*-tagged substrates. Interestingly, a combination of ADP and ATP binding also facilitates *ssrA*-tag binding. For example, when E185Q ClpX hexamers are mixed with sub-saturating concentrations of ATP and an *ssrA*-tag peptide, addition of excess ADP causes a transient increase in *ssrA*-peptide binding followed by eventual dissociation [14]. This result indicates that hexamers with bound ATP and ADP are competent for tag binding.

Comparing the crystal structures of apo and ATP-bound ClpX hexamers show some changes in the axial pore. However, the low resolution of the structures and significant disorder of the pore loops limit useful conclusions about potential conformational changes in this region [18]. When tryptophans were introduced into the pore-1 loop (to generate V154W ClpX), addition of ATP and  $Mg^{++}$  resulted in a red shift in fluorescence, consistent with an increase in solvent accessibility in this region of the enzyme [14].

## 7.3 Lessons from single-chain hexamers

Because ClpX is a homo-hexamer, any mutation affects all six subunits. To allow studies of hexamers with different numbers of active subunits, Martin et al. [23] engineered single-chain molecules in which two, three, or six ClpX<sup>ΔN</sup> coding sequences were genetically linked to produce subunits covalently connected by flexible linkers (Fig. 10A & 10B). Importantly, these molecules formed pseudo hexamers (Fig. 10C) with the same ATP-dependent unfolding and degradation activities as unlinked ClpX<sup>ΔN</sup>. Different numbers of wild-type subunits were then replaced with mutant E185Q or R370K variants to eliminate the ability of those subunits to hydrolyze ATP. Remarkably, a pseudo hexamer with just two opposed wild-type subunits degraded protein substrates at ~30% of the wild-type rate and with the same thermodynamic efficiency, calculated in terms of ATP consumed per substrate degraded (Fig. 10D) [23]. Moreover, a construct with just a single ATP-hydrolysis competent subunit displayed slow but highly specific degradation activity. Thus, protein unfolding and translocation can be powered by ATP hydrolysis in a subset of ClpX subunits, and hydrolysis in just one subunit is sufficient to drive the conformational changes in the enzyme necessary for these mechanical activities.

Single-chain studies also highlight the importance of communication between ClpX subunits. For example, the activities of pseudo-hexamers composed of linked trimers containing wild-type (W), E185Q (E), and R370K (R) subunits change depending on their arrangement within the hexamer [23]. Indeed, the RWE/RWE variant is 8-fold more active in degradation and 3-fold more active in ATP hydrolysis than the WRE/WRE isomer (Fig. 10D). Recall that E185Q subunits in homo-hexamers can adopt ATP-dependent conformations that support ClpP and ssrA-tag binding, whereas R370K subunits do not adopt these conformations. Thus, the activity of a wild-type subunit appears to be enhanced if its clockwise neighbor (the one that donates the large subunit of the shared rigid-body unit) can also undergo nucleotide-dependent conformational changes. E185Q subunits can probably adopt loadable (compatible with ATP binding) or unloadable (incompatible with binding) conformations, whereas R370K subunits may be better suited to the unloadable conformation because of poorer binding to ATP. By this model, ATP-bound ClpX subunits that lie between a nucleotide-free unloadable subunit and a nucleotide-bound loadable subunit probably have the highest hydrolysis activity.

#### 7.4 Unresolved questions about the ATPase cycle

Major questions with respect to the ATPase cycle of ClpX remain unanswered. For example, once four ATPs bind to ClpX, are one, two, three, or four of these nucleotides hydrolyzed before ADP dissociation and ATP rebinding occur? Do subunits with loadable nucleotide-bound conformations convert to unloadable nucleotide-free conformations during the ATPase cycle and *vice versa*? Does ATP hydrolysis in a ClpX hexamer follow any pattern in terms of the order in which specific subunits fire? Models that demand a strict geometric progression (e.g., a subunit fires only after its immediate clockwise neighbor fires) seem to be inconsistent with the observation of functional single-chain hexamers with radically different arrangements of inactive and active subunits [23]. One could argue that the inactive subunits in these hexamers obscure the wild-type pattern because ATP can be removed from an inactive subunit by dissociation rather than hydrolysis. However, this model requires that dissociation from inactive subunits be faster than the overall rate of ATP hydrolysis. In E185Q homo-hexamers, the fastest rate of ATP dissociation is  $\sim 8 \text{ min}^{-1}$ , which is far too slow to account for the WWE/WWE ATP-turnover rate of  $95 \text{ min}^{-1}$  [14,23]. Thus, one would also need to argue that dissociation from E185Q subunits in WWE/WWE occurs faster than in homo-hexamers.

It is also possible that ATP hydrolysis in wild-type ClpX does not follow a regular pattern but is instead probabilistic. For example, after hydrolysis in one subunit, any of the remaining three ATP-bound subunits might fire with distinct probabilities or the same subunit might rebind ATP and fire again, depending upon structural factors and/or interactions with neighboring subunits or a protein substrate. A recent paper argues that probabilistic models are incompatible with communication between subunits [102]. We note, however, that any equilibrium process is inherently probabilistic. The MWC model of allostery, for example, relies upon subunit-subunit communication, but any given oligomer in a population has a fixed probability of assuming the tense or relaxed conformation depending upon the intrinsic equilibrium between these states, ligand binding, and other interactions. [103].

### 8. Translocation and unfolding

Polypeptide translocation is the fundamental mechanical activity of ClpX. Translocation is required to spool unfolded substrates through the axial pore and into the ClpP chamber for degradation. Moreover, translocation of a peptide tag attached to a native protein drives unfolding as ClpX works to pull a large object through its narrow pore.

## 8.1 Pore machinery used for translocation and unfolding

As discussed above, cycles of ATP binding and hydrolysis drive rigid-body movements in the ClpX AAA+ ring. The pore-1 (GYVG) loops in the axial channel of the hexamer are responsible for linking these motions to pulling on the substrate and thus to translocation and unfolding. For example, the V154F mutation in this loop decreases  $V_{\max}$  for degradation of an unfolded substrate ~10 fold, supporting a role in translocation [42]. Furthermore, the Y153A pore-loop mutation eliminated substrate degradation completely, but it was not possible to determine whether this defect involved recognition, unfolding, or translocation.

To understand the Y153A defect in greater depth, this mutation was introduced into just the R subunits, just the W subunits, or just the E subunits of RWE/RWE linked ClpX hexamers [43]. Compared to the parental enzyme, the rates of ATP hydrolysis increased 2-fold or more for each mutant, whether the pore-loop substitutions were in active subunits or inactive subunits. These effects on enzyme “motor speed” indicate that the pore-loop machinery is tightly linked to the ATP-hydrolysis cycle. To adjust for these mutation-induced changes in motor speed, rates of degradation of unfolded or folded substrates can be divided by the working ATPase rate. Strikingly, Y153A substitutions in W or E subunits increased the energetic cost of degradation ~3-fold for unfolded substrate and 10-fold or more for native substrates [43], whereas mutations in the R subunits increased the degradation cost only for folded substrates. This increased cost of degradation suggests that some power strokes of the mutant ClpX enzyme fail to perform useful mechanical work because the mutant pore loops do not grip the substrate polypeptide tightly, do not transmit force efficiently, fail to move the substrate, or allow the polypeptide to slip following a translocation step. Moreover, these effects of GYVG pore-loop mutations on the process of translocation and unfolding strongly support a translocation-induced mechanism of protein denaturation.

## 8.2 Translocation direction, determinants, speed, and step size

There is no compulsory direction of ClpXP degradation, which can initiate at either the N- or C-terminus of a substrate and proceed to the opposite end [28,32,36,39–40,104]. Moreover, translocation does not require recognition by ClpX of specific side chains or peptide-bond spacings, as sequences with homopolymeric stretches of proline, glycine, positively or negatively charged amino acids, aromatic residues, hydrophobic amino acids, D-amino acids, and unnatural residues with additional methylenes between successive amide bonds are all translocated at reasonable rates [105]. These results suggest that ClpX grips translocating substrates largely using van der Waal’s contacts and/or interactions with scattered carbonyl oxygens along the polypeptide chain. Poly-proline cannot form a  $\beta$ -strand or  $\alpha$ -helix, and most other sequences would be unstable in the conformations that poly-proline does adopt. Thus, different segments of unfolded polypeptides are likely to be translocated in different conformations, and the step size for translocation may also vary with sequence.

ClpXP can also initiate degradation at internal substrate sequences and degrade disulfide-bonded substrates, necessitating concurrent translocation of two or more polypeptides through the pore (Fig. 6B) [33,58,106]. How does the ClpX hexamer pull on radically different sequences in single or multiple polypeptides? The pore in the crystal structure of the ClpX hexamer is almost completely closed and would need to expand to grip substrates with large side chains or multiple chains [18,105]. In some sense, this might occur analogously to the unhinging of the jaws of a snake, which allow it to swallow large prey. For example, the hinge between the large and small AAA+ domains of unloadable subunits and the flanking helix of the small domain could unravel to allow the pore to widen to accommodate larger substrates and then refold to allow the pore to reclose and to maintain intimate contacts with smaller substrates (Fig. 11) [18]

Single-molecule and biochemical studies demonstrate that ClpX and ClpXP take translocation steps of 5–8 amino acids, with an average rate of  $\sim 1800$  residues  $\text{min}^{-1}$  [36,107–109]. Translocation is highly processive. For example, translocation of an unfolded filamin domain ( $\sim 100$  residues) occurs in  $\sim 15$  sequential steps without detectable slipping in single molecule studies, except at high resisting loads or low ATP concentrations [36]. Comparing the average rates of ATP hydrolysis and translocation indicates that  $\sim 1$  ATP is hydrolyzed per step. Translocation slows as the ATP concentration is reduced, as ATP $\gamma$ S is added, or as the resisting force increases. Nevertheless, translocation steps of  $\sim 10$  Å are still observed against resisting forces of 20 pN, demonstrating that ClpXP can perform a minimum of 3 kcal/mol of mechanical work per power stroke. The low force-dependence of translocation also suggests that a chemical step rather than a force-dependent step is rate limiting under normal conditions. The ATP-fueled conformational changes that drive translocation and unfolding would be expected to be force-dependent, suggesting that these motions are not rate limiting for ATP hydrolysis.

### 8.3 Unfolding activity, costs, and limits

ClpXP has a robust ability to unfold native proteins with appropriate degradation tags, including *Thermus thermophilus* RNase H\* ( $\Delta G_{\text{unfold}} \sim 12$  kcal/mol), GFP (half-life of years for solution unfolding), and the I27 domain of human titin (AFM denaturation requires  $\sim 200$  pN of force) [11,34–35,110–111]. Importantly, ClpXP degrades native titin<sup>I27-ssrA</sup>  $\sim 16$ -fold slower than an unfolded variant, demonstrating that unfolding is rate limiting for degradation of the folded substrate [34]. In addition, ClpXP degrades N-terminally tagged titin<sup>I27</sup>  $\sim 4$ -fold faster than C-terminally tagged titin<sup>I27</sup> [112], suggesting that pulling on the N terminus and nearby structural elements results in faster unfolding. Matouschek and colleagues [32] originally proposed the idea that AAA+ proteases promote unfolding by pulling on and disrupting local elements of structure [32]. If the stability of local structure is paramount in resisting ClpXP pulling, then neither the global stabilities nor the solution unfolding kinetics of substrate proteins are expected to correlate with the maximal rates at which they are degraded by ClpXP, a result which is frequently observed [35].

Several experiments show that ClpXP successfully unfolds stable protein domains only after numerous failed attempts. (i) An average of  $\sim 500$  ATPs are hydrolyzed by ClpXP during the time needed to unfold a single native titin<sup>I27</sup> molecule [34], indicating that most power strokes do not result in denaturation. (ii) Single-molecule traces of ClpXP degradation of a substrate with multiple filamin domains show dwells between completion of translocation of one domain and unfolding of the next in which the substrate-bound enzyme shows no detectable movement (Fig. 12) [36]. During these dwell periods, ClpX continues to hydrolyze ATP as it attempts to unfold the next domain. Moreover, the pre-unfolding dwell times for any specific domain are exponentially distributed and can vary from a few to several hundred seconds in different experiments. In combination, these results indicate that the proximal local structure of the target domain resists unfolding during most ClpXP power strokes. Occasionally, however, a power stroke will coincide with transient thermal destabilization of this local structure, allowing productive unfolding. When unfolding of a filamin domain does occur in single-molecule experiments, the reaction is complete within a few milliseconds and is generally highly cooperative [36]. This time is far smaller than the average time between ATP-hydrolysis events, providing strong evidence that unfolding, although stochastic, eventually results from a single ATP-dependent power stroke.

Some proteins completely resist ClpXP unfolding. For example, ClpXP cannot degrade methotrexate-bound mouse DHFR or degrade GFP with an N-terminal degradation tag at detectable rates [32,106]. ClpXP unfolding and degradation of GFP from the C-terminus also requires a minimum threshold rate of ATP hydrolysis, suggesting that multiple coordinated hydrolysis events are needed before global unfolding of this substrate occurs



[107]. This result would be expected if one power stroke extracted only the C-terminal strand of this  $\beta$ -barrel substrate, requiring rapid ATP-dependent translocation and subsequent pulling on the remaining structure to guarantee global unfolding. When a protein resists the unfolding force of a ClpXP power stroke, two outcomes are possible. In some cases, the enzyme maintains its grip on the substrate and simply tries again [36]. In other instances, the substrate dissociates upon failed unfolding [32,104]. If dissociation occurs before proteolysis of the degradation tag, then ClpXP can rebind and eventually degrade the substrate. Thus, ClpXP is not committed to degrade an engaged protein that stubbornly resists unfolding, allowing it to preferentially degrade the most easily unfolded proteins in a mixture of substrates [104]. However, dissociation after tag cleavage can generate partially processed proteins that are no longer substrates [32,104]. In the context of a cell, ClpXP and its substrates co-evolve. Therefore, it is unclear if natural substrates are ever processed by ClpXP or generally require as much ATP hydrolysis for unfolding and degradation as is observed for “hyper-stable” model substrates *in vitro*. Nevertheless, ClpXP can unfold and degrade an enormous assortment of proteins with a wide range of structures and stabilities, allowing it to function in protein quality control and numerous regulatory circuits in bacteria and eukaryotic organelles.

## Acknowledgments

We thank the members of our labs and all of those who have contributed to our present understanding of ClpXP. Work in our labs is supported in part from grants from the NIH (AI-15706, AI-16892, GM-499224) and by the Howard Hughes Medical Institute. T.A.B. is an employee of H.H.M.I.

## References

1. Hanson PI, Whiteheart SW. AAA+ proteins: have engine, will work. *Nat Rev Mol Cell Biol.* 2005; 6:519–529. [PubMed: 16072036]
2. Sauer RT, Baker TA. AAA+ proteases: ATP-fueled machines of protein destruction. *Annu Rev Biochem.* 2011 Jun 23. [Epub ahead of print].
3. Katayama-Fujimura Y, Gottesman S, Maurizi MR. A multiple-component, ATP-dependent protease from *Escherichia coli*. *J Biol Chem.* 1987; 262:4477–4485. [PubMed: 3549708]
4. Katayama Y, Gottesman S, Pumphrey J, Rudikoff S, Clark WP, Maurizi MR. The two-component, ATP-dependent Clp protease of *Escherichia coli*. Purification, cloning, and mutational analysis of the ATP-binding component. *J Biol Chem.* 1988; 263:15226–15236. [PubMed: 3049606]
5. Hwang BJ, Woo KM, Goldberg AL, Chung CH. Protease Ti, a new ATP-dependent protease in *Escherichia coli*, contains protein-activated ATPase and proteolytic functions in distinct subunits. *J Biol Chem.* 1988; 263:8727–8734. [PubMed: 2967816]
6. Wojtkowiak D, Georgopoulos C, Zylicz M. Isolation and characterization of ClpX, a new ATP-dependent specificity component of the Clp protease of *Escherichia coli*. *J Biol Chem.* 1993; 268:22609–22617. [PubMed: 8226769]
7. Gottesman S, Clark WP, de Crecy-Lagard V, Maurizi MR. ClpX, an alternative subunit for the ATP-dependent Clp protease of *Escherichia coli*. Sequence and *in vivo* activities. *J Biol Chem.* 1993; 268:22618–22626. [PubMed: 8226770]
8. Levchenko I, Luo L, Baker TA. Disassembly of the Mu transposase tetramer by the ClpX chaperone. *Genes Dev.* 1995; 9:2399–2408. [PubMed: 7557391]
9. Kruklytis R, Welty DJ, Nakai H. ClpX protein of *Escherichia coli* activates bacteriophage Mu transposase in the strand transfer complex for initiation of Mu DNA synthesis. *EMBO J.* 1996; 15:935–944. [PubMed: 8631314]
10. Grimaud R, Kessel M, Beuron F, Steven AC, Maurizi MR. Enzymatic and structural similarities between the *Escherichia coli* ATP-dependent proteases, ClpXP and ClpAP. *J Biol Chem.* 1998; 273:12476–12481. [PubMed: 9575205]

11. Kim YI, Burton RE, Burton BM, Sauer RT, Baker TA. Dynamics of substrate denaturation and translocation by the ClpXP degradation machine. *Mol Cell*. 2000; 5:639–648. [PubMed: 10882100]
12. Wah DA, Levchenko I, Baker TA, Sauer RT. Characterization of a specificity factor for an AAA+ ATPase: Assembly of SspB dimers with ssrA-tagged proteins and the ClpX hexamer. *Chem Biol*. 2002; 9:1237–1245. [PubMed: 12445774]
13. Joshi SA, Hersch GL, Baker TA, Sauer RT. Communication between ClpX and ClpP during substrate processing and degradation. *Nat Struct Mol Biol*. 2004; 11:404–411. [PubMed: 15064753]
14. Hersch GL, Burton RE, Bolon DN, Baker TA, Sauer RT. Asymmetric interactions of ATP with the AAA+ ClpX6 unfoldase: allosteric control of a protein machine. *Cell*. 2005; 121:1017–1027. [PubMed: 15989952]
15. Wojtyra UA, Thibault G, Tuite A, Houry WA. The N-terminal zinc binding domain of ClpX is a dimerization domain that modulates the chaperone function. *J Biol Chem*. 2003; 278:48981–48990. [PubMed: 12937164]
16. Donaldson LW, Wojtyra U, Houry WA. Solution structure of the dimeric zinc binding domain of the chaperone ClpX. *J Biol Chem*. 2003; 278:48991–48996. [PubMed: 14525985]
17. Park EY, Lee BG, Hong SB, Kim HW, Jeon H, Song HK. Structural basis of SspB-tail recognition by the zinc binding domain of ClpX. *J Mol Biol*. 2007; 367:514–526. [PubMed: 17258768]
18. Glynn SE, Martin A, Nager AR, Baker TA, Sauer RT. Crystal structures of asymmetric ClpX hexamers reveal nucleotide-dependent motions in a AAA+ protein-unfolding machine. *Cell*. 2009; 139:744–756. [PubMed: 19914167]
19. Kim DY, Kim KK. Crystal structure of ClpX molecular chaperone from *Helicobacter pylori*. *J Biol Chem*. 2003; 278:50664–50670. [PubMed: 14514695]
20. Neuwald AF, Aravind L, Spouge JL, Koonin EV. AAA+: A class of chaperone-like ATPases associated with the assembly, operation, and disassembly of protein complexes. *Genome Res*. 1999; 9:27–43. [PubMed: 9927482]
21. Erzberger JP, Berger JM. Evolutionary relationships and structural mechanisms of AAA+ proteins. *Annu Rev Biophys Biomol Struct*. 2006; 35:93–114. [PubMed: 16689629]
22. Singh SK, Rozycki J, Ortega J, Ishikawa T, Lo J, Steven AC, Maurizi MR. Functional domains of the ClpA and ClpX molecular chaperones identified by limited proteolysis and deletion analysis. *J Biol Chem*. 2001; 276:29420–29429. [PubMed: 11346657]
23. Martin A, Baker TA, Sauer RT. Rebuilt AAA+ motors reveal operating principles for ATP-fueled machines. *Nature*. 2005; 437:1115–1120. [PubMed: 16237435]
24. Martin A, Baker TA, Sauer RT. Distinct static and dynamic interactions control ATPase-peptidase communication in a AAA+ protease. *Mol Cell*. 2007; 27:41–52. [PubMed: 17612489]
25. Laachouch JE, Desmet L, Geuskens V, Grimaud R, Toussaint A. Bacteriophage Mu repressor as a target for the *Escherichia coli* ATP-dependent Clp protease. *EMBO J*. 1996; 15:437–444. [PubMed: 8617219]
26. Levchenko I, Yamauchi M, Baker TA. ClpX and MuB interact with overlapping regions of Mu transposase: implications for control of the transposition pathway. *Genes Dev*. 1997; 11:1561–1572. [PubMed: 9203582]
27. Neher SB, Villen J, Oakes E, Bakalarski C, Sauer RT, Gygi SP, Baker TA. Proteomic profiling of ClpXP substrates following DNA damage reveals extensive instability within SOS regulon. *Mol Cell*. 2006; 22:193–204. [PubMed: 16630889]
28. Gottesman S, Roche E, Zhou YN, Sauer RT. The ClpXP and ClpAP proteases degrade proteins with C-terminal peptide tails added by the SsrA tagging system. *Genes Dev*. 1998; 12:1338–1347. [PubMed: 9573050]
29. Keiler KC, Waller PRH, Sauer RT. Role of a peptide-tagging system in degradation of proteins translated from damaged mRNA. *Science*. 1996; 271:990–993. [PubMed: 8584937]
30. Moore SE, Sauer RT. The tmRNA system for translational surveillance and ribosome rescue. *Annu Rev Biochem*. 2007; 76:101–124. [PubMed: 17291191]

31. Singh SK, Grimaud R, Hoskins JR, Wickner S, Maurizi MR. Unfolding and internalization of proteins by the ATP-dependent proteases ClpXP and ClpAP. *Proc Natl Acad Sci USA*. 2000; 97:8898–8903. [PubMed: 10922052]
32. Lee C, Schwartz MP, Prakash S, Iwakura M, Matouschek A. ATP-dependent proteases degrade their substrates by processively unraveling them from the degradation signal. *Mol Cell*. 2001; 7:627–637. [PubMed: 11463387]
33. Burton RE, Siddiqui SM, Kim YI, Baker TA, Sauer RT. Effects of protein stability and structure on substrate processing by the ClpXP unfolding and degradation machine. *EMBO J*. 2001; 20:3092–3100. [PubMed: 11406586]
34. Kenniston JA, Baker TA, Fernandez JM, Sauer RT. Linkage between ATP consumption and mechanical unfolding during the protein processing reactions of an AAA+ degradation machine. *Cell*. 2003; 114:511–520. [PubMed: 12941278]
35. Kenniston JA, Burton RE, Siddiqui SM, Baker TA, Sauer RT. Effects of local protein stability and the geometric position of the substrate degradation tag on the efficiency of ClpXP denaturation and degradation. *J Struct Biol*. 2004; 146:130–140. [PubMed: 15037244]
36. Aubin-Tam ME, Olivares AO, Sauer RT, Baker TA, Lang MJ. Single-molecule protein unfolding and translocation by an ATP-fueled proteolytic machine. *Cell*. 2011; 145:257–267. [PubMed: 21496645]
37. Flynn JM, Levchenko I, Seidel M, Wickner SH, Sauer RT, Baker TA. Overlapping recognition determinants within the *ssrA* degradation tag allow modulation of proteolysis. *Proc Natl Acad Sci USA*. 2001; 11:10584–10589. [PubMed: 11535833]
38. Levchenko I, Seidel M, Sauer RT, Baker TA. A specificity-enhancing factor for the ClpXP degradation machine. *Science*. 2000; 289:2354–2356. [PubMed: 11009422]
39. Flynn JM, Neher SB, Kim YI, Sauer RT, Baker TA. Proteomic discovery of cellular substrates of the ClpXP protease reveals five classes of ClpX-recognition signals. *Mol Cell*. 2003; 11:671–683. [PubMed: 12667450]
40. Gonciarz-Swiatek M, Wawrzynow A, Um SJ, Learn BA, McMacken R, Kelley WL, Georgopoulos C, Sliemers O, Zylicz M. Recognition, targeting, and hydrolysis of the lambda O replication protein by the ClpP/ClpX protease. *J Biol Chem*. 1999; 274:13999–14005. [PubMed: 10318812]
41. Martin A, Baker TA, Sauer RT. Diverse pore loops of the AAA+ ClpX machine mediate unassisted and adaptor-dependent recognition of *ssrA*-tagged substrates. *Mol Cell*. 2008; 29:441–450. [PubMed: 18313382]
42. Siddiqui SM, Sauer RT, Baker TA. Role of the protein-processing pore of ClpX, an AAA+ ATPase, in recognition and engagement of specific protein substrates. *Genes Dev*. 2004; 18:369–374. [PubMed: 15004005]
43. Martin A, Baker TA, Sauer RT. Pore loops of the AAA+ ClpX machine grip substrates to drive translocation and unfolding. *Nat Struct Mol Biol*. 2008; 15:1147–1151. [PubMed: 18931677]
44. Farrell CM, Baker TA, Sauer RT. Altered specificity of a AAA+ protease. *Mol Cell*. 2007; 25:161–166. [PubMed: 17218279]
45. Neher SB, Sauer RT, Baker TA. Distinct peptide signals in the UmuD and UmuD' Subunits of UmuD/D' mediate tethering and substrate-processing by the ClpXP protease. *Proc Natl Acad Sci USA*. 2003; 100:13219–13224. [PubMed: 14595014]
46. Gonzalez M, Rasulova F, Maurizi MR, Woodgate R. Subunit-specific degradation of the UmuD/D' heterodimer by the ClpXP protease: the role of trans recognition in UmuD' stability. *EMBO J*. 2000; 19:5251–5258. [PubMed: 11013227]
47. Mhammedi-Alaoui A, Pato M, Gama MJ, Toussaint A. A new component of bacteriophage Mu replicative transposition machinery: the *Escherichia coli* ClpX protein. *Mol Microbiol*. 1994; 11:1109–1116. [PubMed: 8022280]
48. Abdelhakim AH, Oakes ESC, Sauer RT, Baker TA. Unique contacts direct high-priority recognition of the tetrameric transposase-DNA complex by the AAA+ unfoldase ClpX. *Mol Cell*. 2008; 11:39–50. [PubMed: 18406325]
49. Flynn JF, Levchenko I, Sauer RT, Baker TA. Modulating substrate choice: the SspB adaptor delivers a regulator of the extracytoplasmic-stress response to the AAA+ protease ClpXP for degradation. *Genes Dev*. 2004; 18:2292–2301. [PubMed: 15371343]

50. Zhou Y, Gottesman S, Hoskins JR, Maurizi MR, Wickner S. The RssB response regulator directly targets sigma(S) for degradation by ClpXP. *Genes Dev.* 2001; 15:627–637. [PubMed: 11238382]
51. Hengge R. Proteolysis of sigmaS (RpoS) and the general stress response in *Escherichia coli*. *Res Microbiol.* 2009; 160:667–76. [PubMed: 19765651]
52. Levchenko I, Grant RA, Wah DA, Sauer RT, Baker TA. Structure of a delivery protein for a AAA + protease in complex with a peptide degradation tag. *Mol Cell.* 2003; 12:365–372. [PubMed: 14536076]
53. Song HK, Eck MJ. Structural basis of degradation signal recognition by SspB, a specificity-enhancing factor for the ClpXP proteolytic machine. *Mol Cell.* 2003; 12:75–86. [PubMed: 12887894]
54. Wah DA, Levchenko I, Rieckhof GE, Bolon DN, Baker TA, Sauer RT. Flexible linkers leash the substrate-binding domain of SspB to a peptide module that stabilizes delivery complexes with the AAA+ ClpXP protease. *Mol Cell.* 2003; 12:355–363. [PubMed: 14536075]
55. Dougan DA, Weber-Ban E, Bukau B. Targeted delivery of an *ssrA*-tagged substrate by the adaptor protein SspB to its cognate AAA+ protein ClpX. *Mol Cell.* 2003; 12:373–380. [PubMed: 14536077]
56. Bolon DN, Wah DA, Hersch GL, Baker TA, Sauer RT. Bivalent tethering of SspB to ClpXP is required for efficient substrate delivery: a protein-design study. *Mol Cell.* 2004; 13:443–449. [PubMed: 14967151]
57. Hersch GL, Baker TA, Sauer RT. SspB delivery of substrates for ClpXP proteolysis probed by the design of improved degradation tags. *Proc Natl Acad Sci USA.* 2004; 101:12136–12141. [PubMed: 15297609]
58. Bolon DN, Grant RA, Baker TA, Sauer RT. Nucleotide-dependent substrate handoff from the SspB adaptor to the AAA+ ClpXP protease. *Mol Cell.* 2004; 16:343–350. [PubMed: 15525508]
59. Alba BM, Gross CA. Regulation of the *Escherichia coli* sigma-dependent envelope stress response. *Mol Microbiol.* 2004; 52:613–619. [PubMed: 15101969]
60. Chaba R, Grigorova IL, Flynn JM, Baker TA, Gross CA. Design principles of the proteolytic cascade governing the sigmaE-mediated envelope stress response in *Escherichia coli*: keys to graded, buffered, and rapid signal transduction. *Genes Dev.* 2007; 21:124–136. [PubMed: 17210793]
61. Levchenko I, Grant RA, Flynn JM, Sauer RT, Baker TA. Versatile modes of peptide recognition by the AAA+ adaptor protein SspB. *Nat Struct Mol Biol.* 2005; 12:520–525. [PubMed: 15880122]
62. McGinness KE, Baker TA, Sauer RT. Engineering controllable protein degradation. *Mol Cell.* 2006; 22:701–707. [PubMed: 16762842]
63. McGinness KE, Bolon DN, Kaganovich M, Baker TA, Sauer RT. Altered tethering of the SspB adaptor to the ClpXP protease causes changes in substrate delivery. *J Biol Chem.* 2007; 282:11465–11473. [PubMed: 17317664]
64. Griffith KL, Grossman AD. Inducible protein degradation in *Bacillus subtilis* using heterologous peptide tags and adaptor proteins to target substrates to the protease ClpXP. *Mol Microbiol.* 2008; 70:1012–1025. [PubMed: 18811726]
65. Kim JH, Wei JR, Wallach JB, Robbins RS, Rubin EJ, Schnappinger D. Protein inactivation in mycobacteria by controlled proteolysis and its application to deplete the beta subunit of RNA polymerase. *Nucleic Acids Res.* 2011; 39:2210–2220. [PubMed: 21075796]
66. Davis JH, Baker TA, Sauer RT. Engineering synthetic adaptors and substrates for controlled ClpXP degradation. *J Biol Chem.* 2009; 14:21848–21855. [PubMed: 19549779]
67. Moore SD, Sauer RT. Ribosome rescue: tmRNA tagging activity and capacity in *Escherichia coli*. *Mol Micro.* 2005; 58:456–466.
68. Farrell CM, Grossman AD, Sauer RT. Cytoplasmic degradation of *ssrA*-tagged proteins. *Mol Micro.* 2005; 57:1750–1761.
69. Lies M, Maurizi MR. Turnover of endogenous SsrA-tagged proteins mediated by ATP-dependent proteases in *Escherichia coli*. *J Biol Chem.* 2008; 283:22918–22929. [PubMed: 18550539]
70. Pruteanu M, Baker TA. Controlled degradation by ClpXP protease tunes the levels of the excision repair protein UvrA to the extent of DNA damage. *Mol Microbiol.* 2009; 71:912–924. [PubMed: 19183285]

71. Mettert EL, Kiley PJ. ClpXP-dependent proteolysis of FNR upon loss of its O<sub>2</sub>-sensing [4Fe-4S] cluster. *J Mol Biol.* 2005; 354:220–232. [PubMed: 16243354]
72. Brotz-Oesterhelt H, Beyer D, Kroll HP, Endermann R, Ladel C, Schroeder W, Hinzen B, Raddatz S, Paulsen H, Henninger K, Bandow JE, Sahl HG, Labischinski H. Dysregulation of bacterial proteolytic machinery by a new class of antibiotics. *Nat Med.* 2005; 11:1082–1087. [PubMed: 16200071]
73. Kirstein J, Hoffmann A, Lilie H, Schmidt R, Rubsamen-Waigmann H, Brotz-Oesterhelt H, Mogk A, Turgay K. The antibiotic ADEP reprogrammes ClpP, switching it from a regulated to an uncontrolled protease. *EMBO Mol Med.* 2009; 1:37–49. [PubMed: 20049702]
74. Maurizi MR, Clark WP, Katayama Y, Rudikoff S, Pumphrey J, Bowers B, Gottesman S. Sequence and structure of Clp P, the proteolytic component of the ATP-dependent Clp protease of *Escherichia coli*. *J Biol Chem.* 1990; 265:12536–12545. [PubMed: 2197275]
75. Flanagan JM, Wall JS, Capel MS, Schneider DK, Shanklin J. Scanning transmission electron microscopy and small-angle scattering provide evidence that native *Escherichia coli* ClpP is a tetradecamer with an axial pore. *Biochemistry.* 1995; 34:10910–10917. [PubMed: 7662672]
76. Kessel M, Maurizi MR, Kim B, Kocsis E, Trus BL, Singh SK, Steven AC. Homology in structural organization between *E. coli* ClpAP protease and the eukaryotic 26 S proteasome. *J Mol Biol.* 1995; 250:587–594. [PubMed: 7623377]
77. Wang J, Hartling JA, Flanagan JM. The structure of ClpP at 2.3 Å resolution suggests a model for ATP-dependent proteolysis. *Cell.* 1997; 91:447–456. [PubMed: 9390554]
78. Thompson MW, Maurizi MR. Activity and specificity of *Escherichia coli* ClpAP protease in cleaving model peptide substrates. *J Biol Chem.* 1994; 269:18201–18208. [PubMed: 8027081]
79. Thompson MW, Singh SK, Maurizi MR. Processive degradation of proteins by the ATP-dependent Clp protease from *Escherichia coli*. Requirement for the multiple array of active sites in ClpP but not ATP hydrolysis. *J Biol Chem.* 1994; 269:18209–18215. [PubMed: 8027082]
80. Szyk A, Maurizi MR. Crystal structure at 1.9 Å of *E. coli* ClpP with a peptide covalently bound at the active site. *J Struct Biol.* 2006; 156:165–174. [PubMed: 16682229]
81. Kim DY, Kim KK. The structural basis for the activation and peptide recognition of bacterial ClpP. *J Mol Biol.* 2008; 379:760–771. [PubMed: 18468623]
82. Oakes ESC, Sauer RT, Baker TA. unpublished experiments.
83. Lee ME, Baker TA, Sauer RT. Control of substrate gating and translocation into ClpP by channel residues and ClpX binding. *J Mol Biol.* 2010; 399:707–718. [PubMed: 20416323]
84. Kang SG, Maurizi MR, Thompson M, Mueser T, Ahvazi B. Crystallography and mutagenesis point to an essential role for the N-terminus of human mitochondrial ClpP. *J Struct Biol.* 2004; 148:338–352. [PubMed: 15522782]
85. Gribun A, Kimber MS, Ching R, Sprangers R, Fiebig KM, Houry WA. The ClpP double ring tetradecameric protease exhibits plastic ring-ring interactions, and the N termini of its subunits form flexible loops that are essential for ClpXP and ClpAP complex formation. *J Biol Chem.* 2005; 280:16185–16196. [PubMed: 15701650]
86. Bewley MC, Graziano V, Griffin K, Flanagan JM. The asymmetry in the mature amino-terminus of ClpP facilitates a local symmetry match in ClpAP and ClpXP complexes. *J Struct Biol.* 2006; 153:113–128. [PubMed: 16406682]
87. Ingvarsson H, Mate MJ, Høgbom M, Portnoi D, Benaroudj N, Alzari PM, Ortiz-Lombardia M, Unge T. Insights into the inter-ring plasticity of caseinolytic proteases from the X-ray structure of *Mycobacterium tuberculosis* ClpP1. *Acta Crystallogr D Biol Crystallogr.* 2007; 63:249–259. [PubMed: 17242518]
88. Bewley MC, Graziano V, Griffin K, Flanagan JM. Turned on for degradation: ATPase-independent degradation by ClpP. *J Struct Biol.* 2009; 165:118–125. [PubMed: 19038348]
89. Li DH, Chung YS, Gloyd M, Joseph E, Ghirlando R, Wright GD, Cheng YQ, Maurizi MR, Guarné A, Ortega J. Acyldepsipeptide antibiotics induce the formation of a structured axial channel in ClpP: A model for the ClpX/ClpA-bound state of ClpP. *Chem Biol.* 2010; 17:959–969. [PubMed: 20851345]

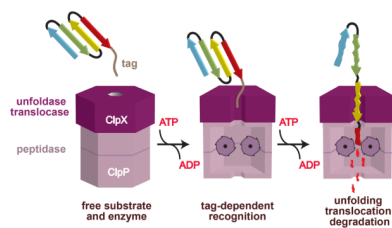


90. Lee BG, Park EY, Lee KE, Jeon H, Sung KH, Paulsen H, Rübsamen-Schaeff H, Brötz-Oesterhelt H, Song HK. Structures of ClpP in complex with acyldepsipeptide antibiotics reveal its activation mechanism. *Nat Struct Mol Biol.* 2010; 17:471–478. [PubMed: 20305655]
91. Yu AY, Houry WA. ClpP: a distinctive family of cylindrical energy-dependent serine proteases. *FEBS Lett.* 2007; 581:3749–3757. [PubMed: 17499722]
92. Maurizi MR, Singh SK, Thompson MW, Kessel M, Ginsburg A. Molecular properties of ClpAP protease of *Escherichia coli*: ATP-dependent association of ClpA and ClpP. *Biochemistry.* 1998; 37:7778–7786. [PubMed: 9601038]
93. Kang SG, Dimitrova MN, Ortega J, Ginsburg A, Maurizi MR. Human mitochondrial ClpP is a stable heptamer that assembles into a tetradecamer in the presence of ClpX. *J Biol Chem.* 2005; 280:35424–35432. [PubMed: 16115876]
94. Kimber MS, Yu AY, Borg M, Leung E, Chan HS, Houry WA. Structural and theoretical studies indicate that the cylindrical protease ClpP samples extended and compact conformations. *Structure.* 2010; 18:798–808. [PubMed: 20637416]
95. Sprangers R, Gribun A, Hwang PM, Houry WA, Kay LE. Quantitative NMR spectroscopy of supramolecular complexes: dynamic side pores in ClpP are important for product release. *Proc Natl Acad Sci USA.* 2005; 102:16678–16683. [PubMed: 16263929]
96. Ortega J, Singh SK, Ishikawa T, Maurizi MR, Steven AC. Visualization of substrate binding and translocation by the ATP-dependent protease, ClpXP. *Mol Cell.* 2000; 6:1515–1521. [PubMed: 11163224]
97. Ortega J, Lee HS, Maurizi MR, Steven AC. Alternating translocation of protein substrates from both ends of ClpXP protease. *EMBO J.* 2002; 21:4938–4949. [PubMed: 12234933]
98. Jennings LD, Bohon J, Chance MR, Licht S. The ClpP N-terminus coordinates substrate access with protease active site reactivity. *Biochemistry.* 2008; 47:11031–11040. [PubMed: 18816064]
99. Kim YI, Levchenko I, Fraczkowska K, Woodruff RV, Sauer RT, Baker TA. Molecular determinants of complex formation between Clp/Hsp100 ATPases and the ClpP peptidase. *Nat Struct Biol.* 2001; 8:230–233. [PubMed: 11224567]
100. Jones JM, Welty DJ, Nakai H. Versatile action of *Escherichia coli* ClpXP as protease or molecular chaperone for bacteriophage Mu transposition. *J Biol Chem.* 1998; 273:459–65. [PubMed: 9417104]
101. Burton RE, Baker TA, Sauer RT. Energy-dependent degradation: Linkage between ClpXP-catalyzed nucleotide hydrolysis and protein-substrate processing. *Protein Sci.* 2003; 12:893–902. [PubMed: 12717012]
102. Smith DM, Fraga H, Reis C, Kafri G, Goldberg AL. ATP binds to proteasomal ATPases in pairs with distinct functional effects, implying an ordered reaction cycle. *Cell.* 2011; 144:526–538. [PubMed: 21335235]
103. Monod J, Wyman J, Changeux JP. On the nature of allosteric transitions: a plausible model. *J Mol Biol.* 1965; 12:88–118. [PubMed: 14343300]
104. Kenniston JA, Baker TA, Sauer RT. Partitioning between unfolding and release of native domains during ClpXP degradation determines substrate selectivity and partial processing. *Proc Natl Acad Sci USA.* 2005; 102:1390–1395. [PubMed: 15671177]
105. Barkow SR, Levchenko I, Baker TA, Sauer RT. Polypeptide translocation by the AAA+ ClpXP protease machine. *Chem Biol.* 2009; 16:605–612. [PubMed: 19549599]
106. Hoskins JR, Yanagihara K, Mizuuchi K, Wickner S. ClpAP and ClpXP degrade proteins with tags located in the interior of the primary sequence. *Proc Natl Acad Sci USA.* 2002; 99:11037–11042. [PubMed: 12177439]
107. Martin A, Baker TA, Sauer RT. Protein unfolding by a AAA+ protease: critical dependence on ATP-hydrolysis rates and energy landscapes. *Nat Struct Mol Biol.* 2008; 15:139–145. [PubMed: 18223658]
108. Shin Y, Davis JH, Brau RR, Martin A, Kenniston JA, Baker TA, Sauer RT, Lang MJ. Single-molecule denaturation and degradation of proteins by the AAA+ ClpXP protease. *Proc Natl Acad Sci USA.* 2009; 106:19340–19345. [PubMed: 19892734]

109. Maillard RA, Chistol G, Sen M, Righini M, Tan J, Kaiser CM, Hodges C, Martin A, Bustamante C. ClpX(P) Generates Mechanical Force to Unfold and Translocate Its Protein Substrates. *Cell*. 2011; 145:459–469. [PubMed: 21529717]
110. Hollien J, Marqusee S. Structural distribution of stability in a thermophilic enzyme. *Proc Natl Acad Sci USA*. 1999; 96:13674–13678. [PubMed: 10570131]
111. Li H, Carrion-Vasquez M, Oberhauser AF, Marszalek PE, Fernandez JM. Point mutations alter the mechanical stability of immunoglobulin modules. *Nat Struct Biol*. 2000; 7:1117–1120. [PubMed: 11101892]
112. Kenniston, JA. PhD thesis. Massachusetts Institute of Technology; Cambridge, MA: 2005. Substrate denaturation and translocation by a proteolytic machine.
113. Sauer RT, Bolon DN, Burton BM, Burton RE, Flynn JM, Grant RA, Hersch GL, Joshi SA, Kenniston JA, Levchenko I, Neher SB, Oakes ESC, Siddiqui SM, Wah DA, Baker TA. Sculpting the proteome with AAA+ proteases and disassembly machines. *Cell*. 2004; 119:9–18. [PubMed: 15454077]

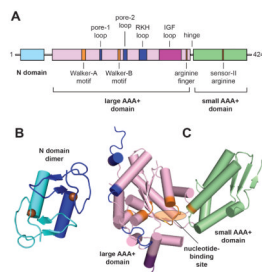
### Research highlights

- Ring hexamers of ClpX unfold and then translocate proteins into ClpP for degradation
- A narrow pore restricts ClpP activity unless ClpX/ClpA or acyldepsipeptides bind
- ClpX recognizes peptide tags or degrons in protein substrates and adaptor proteins
- Asymmetric ATP hydrolysis by one ClpX subunit powers mechanical protein unfolding
- Crystallography and single-molecule results reveal detailed aspects of mechanism



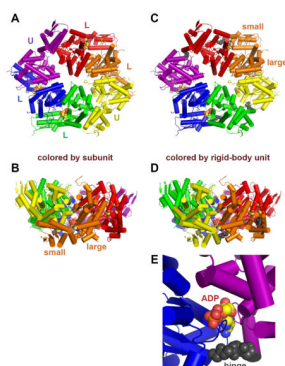
**Fig. 1.**

Cartoon model of substrate recognition and degradation by the ClpXP protease. In an initial recognition step, a peptide tag in a protein substrate binds in the axial pore of the ClpX hexamer. In subsequent ATP-dependent steps, ClpX unfolds the substrate and translocates the unfolded polypeptide into the degradation chamber of ClpP for proteolysis, where it is cleaved into small peptide fragments. Adapted with permission from ref. [113].

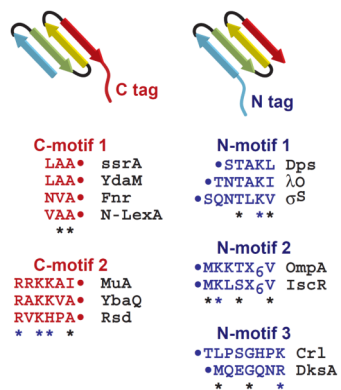


**Fig. 2.** Domain structure of ClpX. **(A)** Arrangement of domains and characteristic functional motifs with respect to the linear sequence are shown for *E. coli* ClpX. Motifs are colored blue for ssrA-tag binding, orange for ATP binding and hydrolysis (orange), or purple for ClpP binding. The pore-2 loop is also involved in ClpP binding. **(B)** Structure of the N-domain dimer (10VX) [16]. Spheres represent zinc atoms. **(C)** Structure of a AAA+ module in a single ClpX subunit (3HWS) [18]. Nucleotide binds in the cleft between the large and small AAA+ domains. Motif colors correspond to those in panel A.



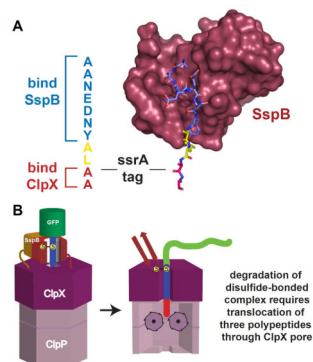


**Fig. 3.** ClpX hexamer structures (3HWS). **(A)** Face view (substrate side) colored by subunits. Nucleotide loadable (L) and unloadable (U) subunits are marked. **(B)** Side view (substrate side up) colored by subunit. **(C)** Face view (substrate side) colored by rigid-body units. **(D)** Side view (substrate side up) colored by rigid-body units. **(E)** Close up of nucleotide-binding site and hinge between two rigid-body units. In each panel, the polypeptide backbone of the hinge region and ADP are shown in CPK representation, whereas most of the protein is shown in cartoon representation.

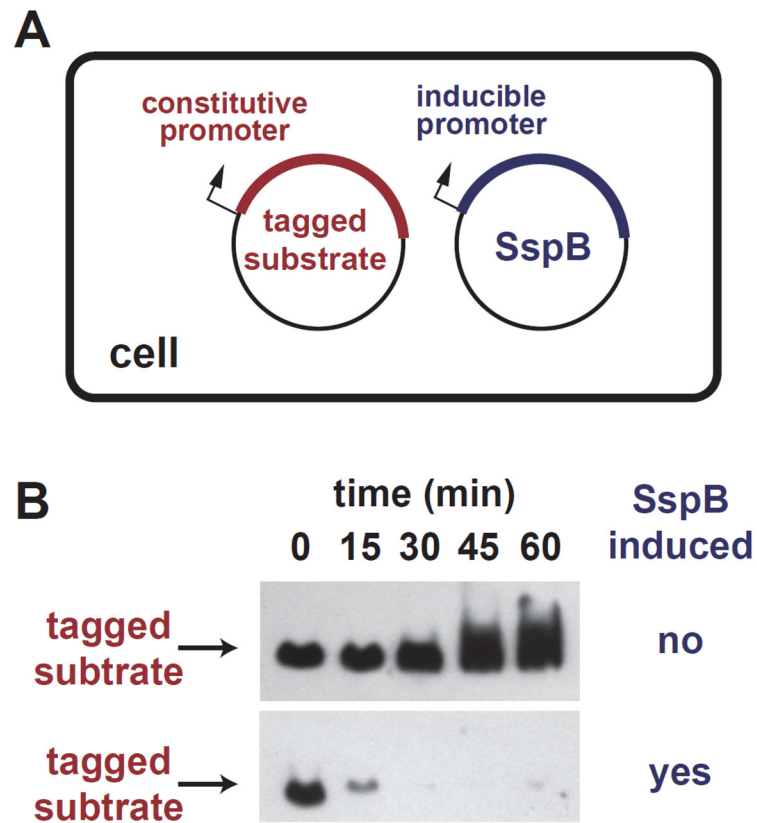


**Fig. 4.** C-terminal and N-terminal sequence tags that target substrates for ClpXP degradation [39]. Red dots –  $\alpha$ -carboxyl group. Blue dots –  $\alpha$ -amino group of mature protein.

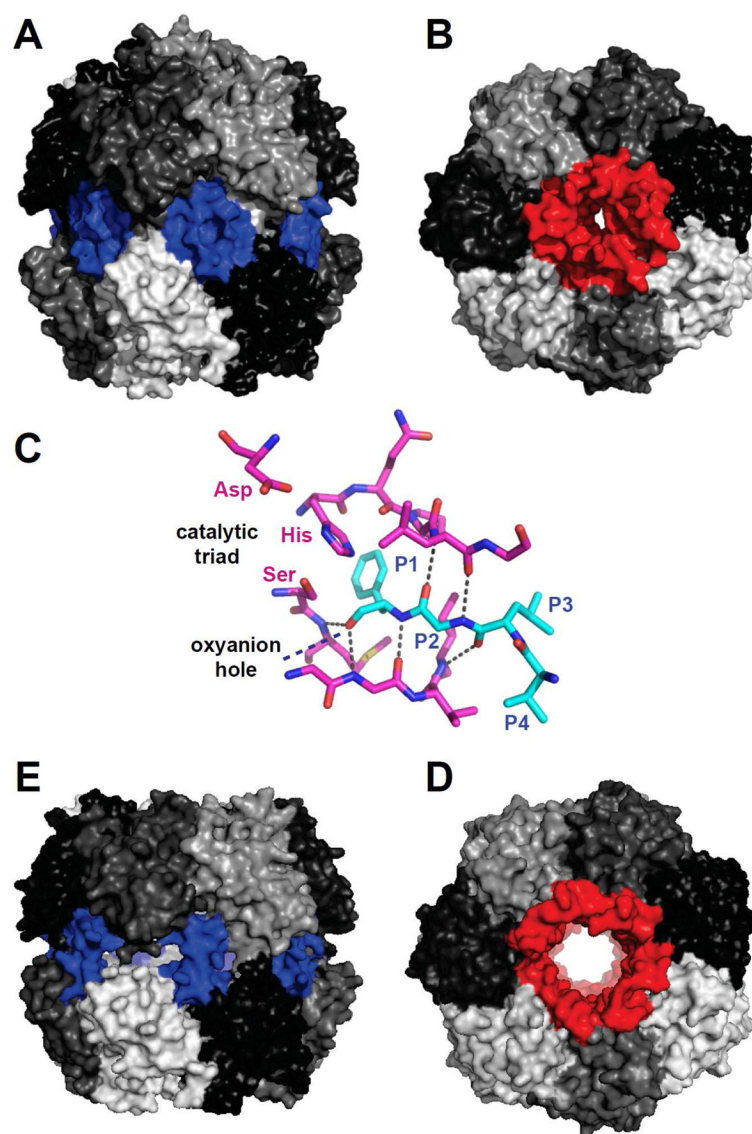




**Fig. 6.** SspB delivers ssrA-tagged substrates to ClpXP. **(A)** SspB (surface representation; 1OU8) binds to the AANDENY portion of the ssrA tag [37,52]. The C-terminal AA-COOH of the tag binds ClpX. **(B)** When SspB is disulfide bonded to the ssrA tag of a GFP substrate, both the adapter and substrate are degraded, requiring concurrent translocation of 3 polypeptides through the ClpX pore. Adapted with permission from ref. [58].

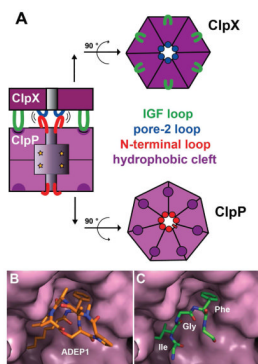


**Fig. 7.** Adaptor-mediated degradation. **(A)** A bacterial cell expresses a substrate with a weak ClpXP-degradation tag constitutively and expresses the SspB adaptor under conditional IPTG control. **(B)** Western blots show that the tagged substrate accumulates over time when SspB is not induced but is degraded rapidly upon induction of SspB synthesis. Adapted with permission from ref. [62].



**Fig. 8.** Structures of ClpP. (A) ClpP (1YG6) contains 14 subunits, arranged as two stacked heptameric rings [77,86]. Interactions between residues 125–146 (blue) in the handle region help stabilize the 14-mer. (B) The axial pore in free ClpP (1YG6) is very narrow, allowing entry of only small peptides into the internal proteolytic chamber. The pore dimensions are established by residues 1–21 (red), which form stem-loop structures. (C) Active site of a ClpP subunit (magenta; 2ZL2) with a bound peptide product (cyan) [81]. Residues of the Ser-His-Asp catalytic triad are labeled and the oxyanion hole is marked. The P1 side chain of the substrate (phenylalanine) sits in a hydrophobic cavity. (D) Acyldepsipeptide binding increases the size of the axial pore (3MT6), allowing degradation of unfolded proteins by ClpP alone [73,89–90]. (E) ClpP can exist in a more compact structure (3HLN) in which the active-site residues assume non-functional conformations are disordered and a portion of the handle region is disordered [91,94].



**Fig. 9.**

Interaction of ClpX and ClpP. (A) The ClpXP complex is stabilized by peripheral interactions between the IGF loops of ClpX and hydrophobic clefts on ClpP, as well as by axial interactions between the pore-2 loops of ClpX and the N-terminal stem-loop of ClpP. Adapted with permission from ref. [24]. (B) Structure of an acyldepsipeptide (ADEP1; stick representation; 3MT6) bound in one of the ClpP clefts (surface representation) [89]. (C) Model of the ClpX IGF peptide binding in the ClpP cleft in a manner analogous to ADEP1.

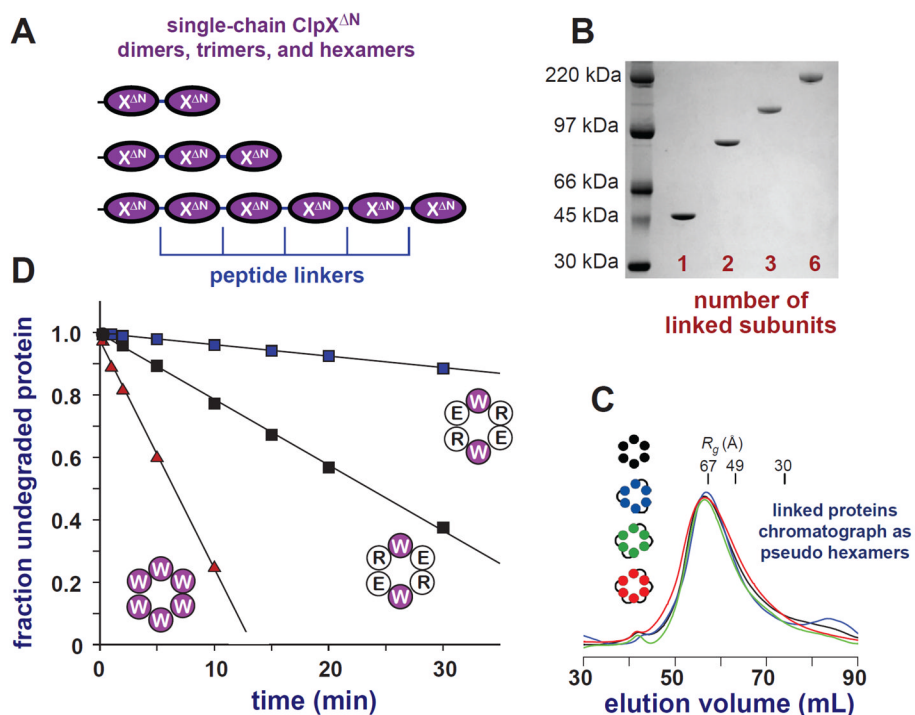


**Fig. 10.** Single-chain ClpX<sup>ΔN</sup> hexamers [23]. **(A)** Two, three, or six ClpX<sup>ΔN</sup> subunits can be connected by peptide linkers [23]. **(B)** SDS-PAGE of purified ClpX<sup>ΔN</sup> proteins containing 1, 2, 3, or 6 linked subunits. **(C)** Unlinked ClpX<sup>ΔN</sup> and linked proteins chromatograph at the position expected for hexamers or pseudo hexamers in gel-filtration chromatography. **(D)** ClpP-mediated degradation of an ssrA-tagged substrate by single-chain hexamers with different numbers of wild-type subunits (W) and/or subunits defective in ATP hydrolysis (E or R). Note that the RWE/RWE hexamer is far more active than the EWR/EWR isomer.

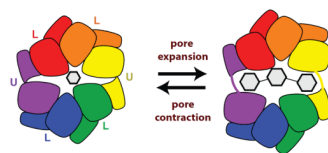


**Fig. 11.**

Expansion and contraction of the axial pore by a snake-jaws model in which pore size is controlled by the size of the substrates and the conformation of the hinge region and flanking structure of the unloadable (U) ClpX subunits.

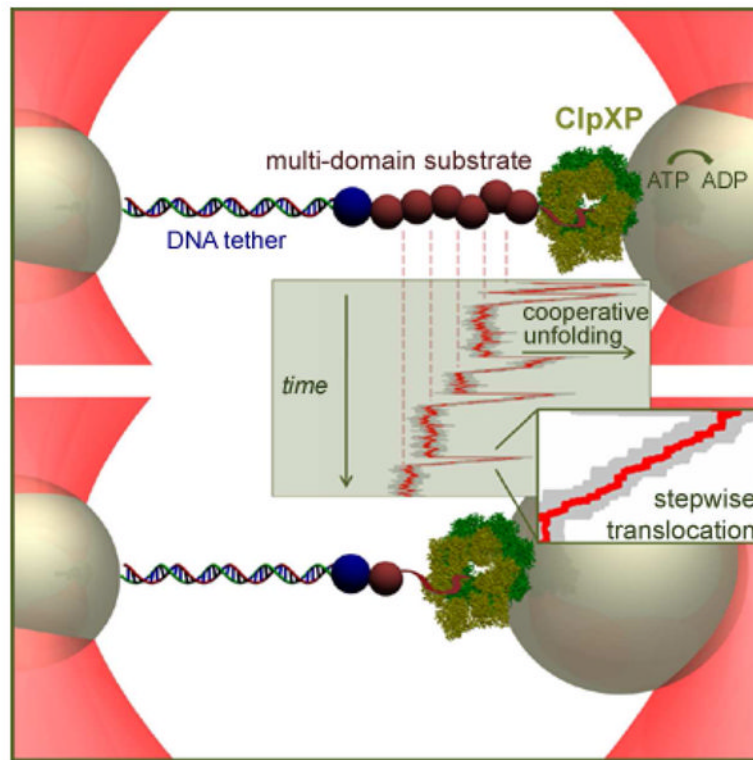


**Fig. 12.** Single-molecule unfolding and translocation of a multi-domain filamin substrate assayed by optical trapping nanometry [36]. Beads attached to substrate or ClpXP are trapped in laser beams. The distance between beads changes as ClpXP denatures or translocates a domain. In the trace shown in the center of the panel, horizontal movements to the right correspond to highly cooperative unfolding in single domains. Subsequent diagonal movements back to the left correspond to translocation. The inset shows that translocation occurs in steps of  $\sim 10$  Å. In the dwell time between completion of translocation of one domain and unfolding of the next domain, the length of the substrate does not change. Adapted with permission from ref. [36].